ANALYTICAL STUDY ON BEHAVIOR OF EXTREMELY SMALL SCALED RC MODELS UNDER SEISMIC LOADINGS

Noriko TOKUI[1], Yoshiaki NAKANO[2], and Noriyuki TAKAHASHI[3]

ABSTRACT: To establish a simple and cost effective testing technique to investigate seismic behaviors of reinforced concrete structures, extremely small scaled model structures consisting of high performance fiber reinforced cement composite (HPFRCC) material reinforced solely with longitudinal reinforcement are fabricated, and their dynamic behaviors are experimentally and analytically investigated.

Key Words: Reinforced concrete, Shaking table test, Scaled model, HPFRCC

INTRODUCTION

Shaking table tests have been widely applied to investigate dynamic behaviors of structures under earthquake excitations. In the shaking table tests of reinforced concrete (R/C) structures, relatively large specimens are generally tested to eliminate difficulties in fabricating specimens. However, the number of shaking tables that have enough capacity to carry out large-scale tests is limited, and much cost and time are generally required. Even when shaking table tests using relatively small specimen are carried out, it may be difficult to provide lateral reinforcement in such a scaled specimen. Another methodology is therefore needed to carry out shaking table tests under limited cost and time.

Recent investigations on high performance fiber reinforced cement composite (HPFRCC) material indicate that tension stiffening as well as multiple cracking effects of HPFRCC may result in its ductile behavior[1)2)]. To establish a simple and cost effective testing technique to investigate seismic behaviors of R/C structures, extremely small scaled model structures consisting of HPFRCC material reinforced solely with longitudinal reinforcement are fabricated, and their dynamic behaviors are experimentally and analytically investigated.

TEST SPECIMENS

In this study, two types of column specimens are designed as shown in Figure 1; Type-S (stub) specimen has stubs at both top and bottom ends, and Type-P (plate) specimen has steel plates at both ends. They are subjected to different loadings, i.e., dynamic excitations and static load reversals. Specimens are referred to as SD, SS, PD and PS, respectively reflecting the end details and loading types as shown below.

Dynamic	Static	Dynamic	Static
SD	SS	PD	PS
Stub	Stub	Plate	Plate

[1] Graduate Student, Graduate School of Engineering, The University of Tokyo,
[2] Professor, Institute of Industrial Science, The University of Tokyo, Dr. Eng.
[3] Research Associate, Institute of Industrial Science, The University of Tokyo, Dr. Eng.

Each specimen has a cross section of 30 x 30 mm and the height of 180 mm. The shear-span-to-depth ratio of each specimen is 3.0 and the tensile reinforcement ratio is 2.19%.

Extremely small-scaled column specimens investigated in this study are not the simply size-reduced models of existing full-scale R/C members but those consisting of longitudinal steel reinforcement and HPFRCC material without lateral reinforcement. As they do not have transverse reinforcement, very small-scaled specimens can be made with less work and lower cost. This method therefore may enable to conduct shaking table tests of simple structures under various sets of input ground motions or those of multi-storied and spanned buildings, which have been generally difficult to perform with ordinary scaled specimens.

Tables 1 and 2 summarize the material properties of HPFRCC and longitudinal reinforcement bars. The HPFRCC is mortar matrix (water-cement ratio: 45%, and sand-cement ratio: 40%) mixed with 1.0% volume ratio of polyethylene fiber (15mm long with a diameter of 12 μm). The cylinder size of material tests is 100mm x 200mm (diameter x height). The longitudinal reinforcement used in the specimens is metric coarse screw threads with a major diameter of external thread of 4mm. The detailed information of screw threads can be found in the Japanese Industrial Standards (JIS) B 0205[3].

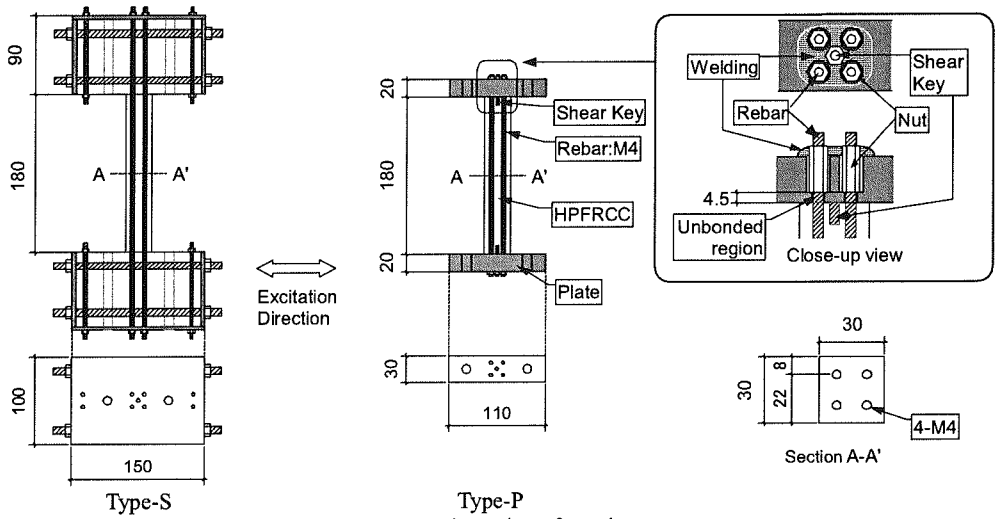

Figure 1. Dimension of specimen

Table 1. Material properties of HPFRCC

Specimen	Age (day)	Young's Modulus*1 E_c(N/mm^2)	Compressive Strength σ_B(N/mm^2)	Strain at Compressive Strength ε_B(%)	Tensile Strength σ_t(N/mm^2)
SD	19	1.95×10^4	45.7	0.34	2.00
SS	16	1.75×10^4	48.7	0.42	-*2
PD	18	1.69×10^4	47.7	0.40	2.14
PS					

*1 secant modulus at 1/3 σ_B

*2 not measured

Table 2. Material properties of longitudinal reinforcement

	Cross Section Area (mm^2)	Young's Modulus E_s(N/mm^2)	Compressive Strength σ_B(N/mm^2)
M4	9.87	1.55×10^5	412

SHAKING TABLE TEST

Test Setup

Test setup is shown in Figure 2. Each specimen is placed on and fixed to component (c). This system has horizontal and vertical sliders, which enable specimens to deform in the lateral and axial direction when they are subjected to anti-symmetric bending during excitations. The relative displacement y between point (a) and component (c) is measured in the direction of excitation. Accelerometers are installed at point (a), (d), and the shaking table. Load cells (1) and (2) are installed at both ends of the component (c), which is placed on the horizontal sliders, to directly evaluate the inertia force acting on the specimen. The inertia force Q of each specimen is calculated from Eqs. (1) and (2) based on the measured force shown in Figure 3. These data are recorded with a sampling interval of 0.002 seconds.

$$Q - P_C + (P_{L1} - P_{L2} - P_{DS}) = 0 \tag{1}$$

$$P_C = m_c a_c$$

Assuming $P_{DS} \approx 0$

$$Q \approx (-P_{L1} + P_{L2}) + m_c a_c \tag{2}$$

where, P_C is the inertia force acting on the lower stub and component (c); m_c and a_c are their mass and absolute acceleration, respectively; P_{L1} and P_{L2} are the forces measured with load cells (1) and (2), respectively; and P_{DS} is the damping force due to the slider.

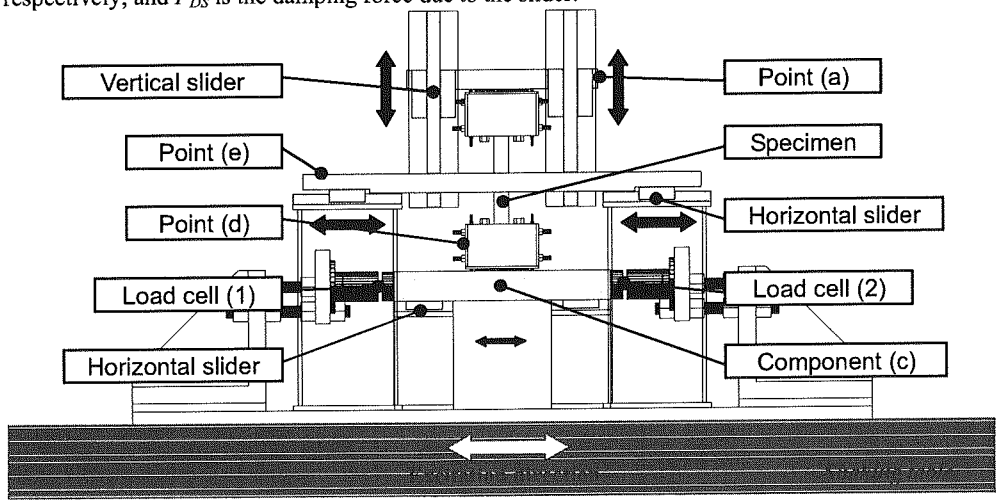

Figure 2. Test setup

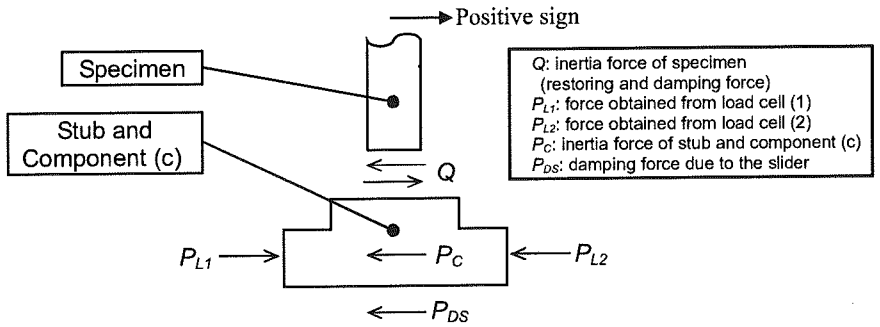

Figure 3. Inertia force of specimen and measured force

Test Program

The calculated initial period of the specimen is 0.074 seconds (the overall weight W of a specimen including self-weight and equipment weight is 3234N and the initial stiffness of a specimen is 2700 kN/mm). The sinusoidal wave of which amplitude increases gradually as shown in Figure 4 is used to excite specimens. The period of the sinusoidal wave is 0.2 seconds, which is about 3 times of the calculated period of specimens.

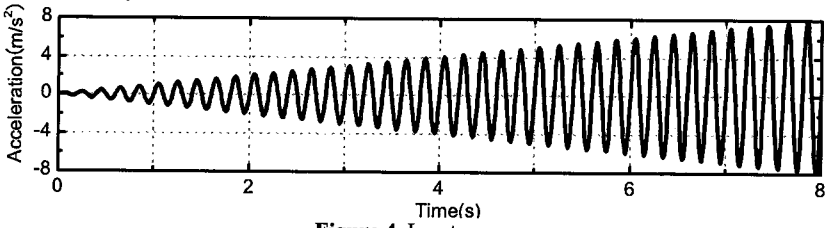

Figure 4. Input wave

Test Result

Figure 5 shows the relationship of response inertia forces Q defined by Eq. (2) and relative displacement y of each specimen. Both specimens show ductile behaviors with spindle shaped hysteresis loops. The maximum inertia force Q_{MAX} of Type-S specimen (SD: 2285N) is 20% larger than that of Type-P specimen (PD: 1897N) although they have the same sectional and material properties. To understand the different Q_{MAX} values, static loading tests of both specimens are carried out and their fundamental behaviors are carefully investigated in the next section.

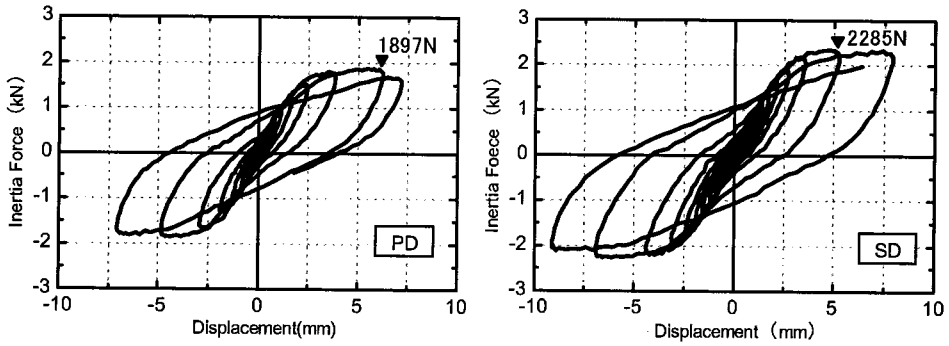

Figure 5. Shaking table test results

STATIC LOADING TEST

In the shaking table tests, as stated earlier, the maximum inertia force Q_{MAX} of Type-S specimen is 20% larger than that of Type-P specimen although they have the same sectional and material properties. To clarify the difference in Q_{MAX} values, static loading tests of both specimens are carried out.

Specimen and Test Setup

The specimens used in the static loading tests are the same as those of shaking table tests. For the static tests, the equipment shown in Figure 6 is attached at point (e) indicated in Figure 2. The displacements obtained in the shaking table tests are applied to each specimen by pushing and pulling point (e). The displacements are imposed with a PC rod by tightening and loosening a nut placed at the reaction wall. After the maximum displacement experienced during the shaking table tests is imposed, each specimen is monotonically loaded to collapse.

Test Result

Figure 7 shows the relationship of restoring force Q and relative displacement y of each specimen. Table 3 shows the maximum restoring force Q_{MAX} of specimens at the displacement where the

specimen PD or SD reached the maximum inertia force Q_{MAX} during shaking table tests shown in Figure 5.

As can be found in Table 3, Q_{MAX} during the shaking table tests is 8% larger for Type-S specimen while it is almost the same for Type-P specimen. This result implies that the effect of strain rate can be different in Type-S and Type-P specimens.

Table 3 also shows that Q_{MAX} of Type-S specimen during the static loading tests is 11% larger than that of Type-P specimen. The larger strength in Type-S specimen may be attributed to the different design details at specimen ends; the Type-S specimen has HPFRCC stub ends where the fiber reinforced cement is monolithically cast together with its mid-column part and the critical sections at both ends can therefore resist tensile actions to some extent even in the post-crack stage, while the Type-P specimen has steel plate ends and they do not contribute to the tensile resistance once the critical section cracks at the interface between the plate and HPFRCC.

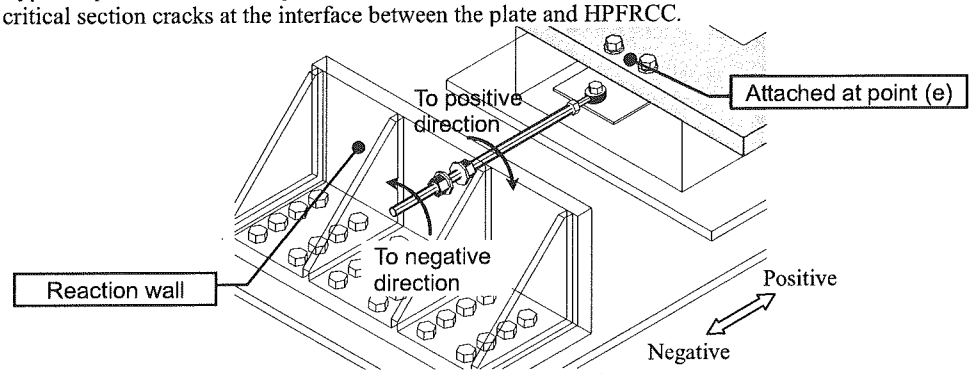

Figure 6. Static loading equipment

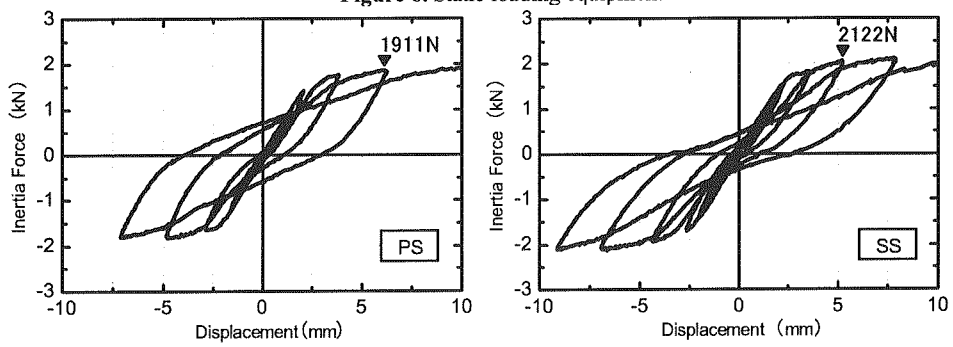

Figure 7. Static loading test results

Table 3. Comparison of maximum Q value (Q_{MAX})

Type of Specimen	Q_{MAX} (N)		(Dynamic Test) / (Static Test)
	Dynamic Test	Static Test	
Type - S	2285 (SD)	2122 (SS)	1.08
Type - P	1897 (PD)	1911 (PS)	0.99
(Type – S) / (Type – P)	1.2	1.11	-

FIBER MODEL ANALYSIS

To investigate the differences in Q_{MAX}, fiber model analyses are carried out considering design details at specimen ends and strain rate effects.

Basic Assumptions in Computation

A triangular curvature distribution is assumed along the test section in both types of specimens. The

location of the neutral axis and the strain of each fiber segment are determined based on the curvature ϕ at the critical section, the equilibrium condition of axial force of a section, and the plane section assumption.

Computation Procedure of Curvature at Critical Section

In the case of Type-S specimen, the curvature ϕ at the critical section to a given displacement y is determined as Eq. (3).

$$\phi = 3y / h^2 \tag{3}$$

where, ϕ : curvature at the critical section,
y : overall displacement,
h : height of specimen.

In the case of Type-P specimen, the longitudinal reinforcement is unbonded over the length of L (4.5mm) in the end plates as shown in Figure 8, and the displacement D_p due to the elongation of longitudinal reinforcement over the unbonded region contributes to the overall displacement y as well as the flexural displacement D_m as shown in Eq. (4).

$$y = D_p + D_m \tag{4}$$

where, D_p : displacement due to the elongation of longitudinal reinforcement,
D_m : flexural displacement.

The contribution of D_p and D_m to overall displacement y is determined in the following manner.

1) Assume $D_m = y$.

2) Determine the curvature ϕ at the critical section as is made for Type-S specimen.

$$\phi = 3\, D_m / h^2 \tag{5}$$

3) Determine the location of neutral axis x_n from the extreme tensile fiber.

4) Calculate strain ε of longitudinal reinforcement at the critical section.

$$\varepsilon = \phi \cdot x_n + \varepsilon_0 \tag{6}$$

where, ε : stain of longitudinal reinforcement at the critical section,
x_n : distance from the extreme tensile fiber to neutral axis,
ε_0 : stain due to axial force.

5) Assume $\varepsilon_p = \varepsilon$.
where, ε_p : stain of longitudinal reinforcement at the unbonded region.

6) Calculate the elongation δ over unbonded region.

$$\delta = \varepsilon_p \cdot L \tag{7}$$

where, δ : elongation of longitudinal reinforcement at the unbonded region,
L : length of unbonded region in the end plate (=4.5mm).

7) Calculate the rotational angle θ at the critical section.

$$\theta = \delta / (x_n - d_t) \tag{8}$$

where, θ : rotational angle due to elongation of longitudinal reinforcement,
d_t : distance from extreme tensile fiber to the centroid of tension reinforcement.

8) Calculate the displacement D_p due to the elongation of longitudinal reinforcement

$$D_p = \theta \cdot h \tag{9}$$

9) Compare y with $D_m + D_p$.
If not converged, increase or decrease in D_m and go to 2).

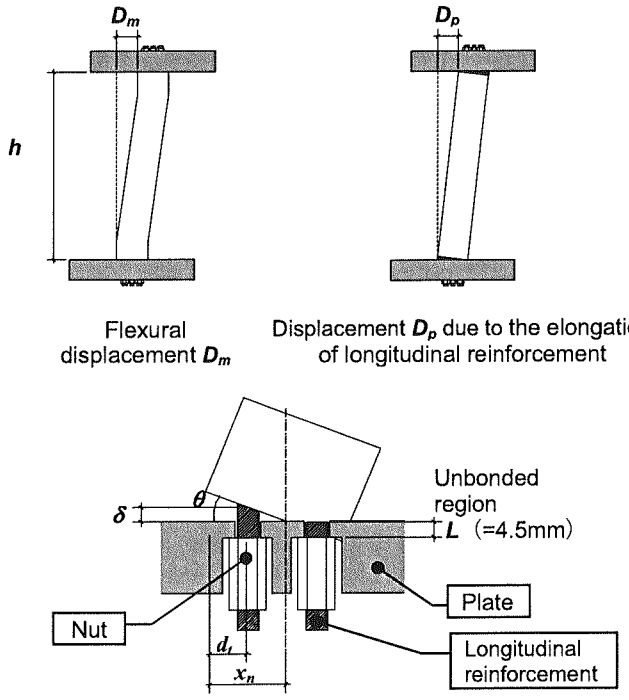

Figure 8. Displacement definition of Type-P specimen

Strain Rate Effect on Material Characteristics

The strain rate $\dot{\varepsilon}_i$ at i-th step, which is calculated by Eq. (10), is considered to incorporate its effect on material stiffness and strength.

$$\dot{\varepsilon}_i = (\varepsilon_i - \varepsilon_{i-1}) / (t_i - t_{i-1}) \tag{10}$$

where, ε_i : strain at i-th step,
t_i : time at i-th step.

Figure 9 shows material properties model for HPFRCC and longitudinal reinforcement under static loadings. In compression, the σ - ε relation of HPFRCC is represented with (1) a linear line having a slope of the initial Young's modulus E_c and (2) an exponential function curve that passes through the origin (0, 0) and the peak (ε_B, σ_B). In tension, a cracked section is assumed to maintain the tensile strength of $0.05 \times \sigma_B$ up to 2% in strain for Type-S specimen, while the strength contribution is neglected for Type-P specimen. The Young's modulus E_c and strength σ_B shown in Table 1 is then factored in accordance with the strain rate $\dot{\varepsilon}$ under dynamic loadings, as shown in Eqs. (11) through (16). In both tension and compression, the σ - ε relation of longitudinal reinforcement is represented with Ramberg-Osgood model ($\alpha = 1$, $\gamma = 12$). The yield strength σ_y shown in Table 2 is factored in accordance with the strain rate $\dot{\varepsilon}$, as shown in Eqs. (17) and (18).

(a)HPFRCC

young's modulus

$|\dot{\varepsilon}| > 10^1 \mu/sec$

$$ {}_dE_C = (0.02 log|\dot{\varepsilon}| + 0.98)\, {}_sE_C \quad (11) $$

$|\dot{\varepsilon}| \leqq 10^1 \mu/sec$

$$ {}_dE_C = {}_sE_C \quad (12) $$

where, ${}_dE_C$: Young's modulus of HPFRCC (under dynamic loading)

${}_sE_C$: Young's modulus of HPFRCC (under static loading)

compressive strength

$|\dot{\varepsilon}| > 10^1 \mu/sec$

$$ {}_d\sigma_B = (0.06 log|\dot{\varepsilon}| + 0.94)\, {}_s\sigma_B \quad (13) $$

$|\dot{\varepsilon}| \leqq 10^1 \mu/sec$

$$ {}_d\sigma_B = {}_s\sigma_B \quad (14) $$

where, ${}_d\sigma_B$: compressive strength of HPFRCC (under dynamic loading)

${}_s\sigma_B$: compressive strength of HPFRCC (under static loading)

tensile strength

In the case of Type-S

$$ \sigma_t = {}_d\sigma_B / 20 \quad (15) $$

In the case of Type-P

$$ \sigma_t = 0 \quad (16) $$

where, σ_t : tensile strength of HPFRCC

(b)Longitudinal Reinforcement

yield strength of longitudinal reinforcement

$|\dot{\varepsilon}| > 10^2 \mu/sec$

$$ {}_df_y = (0.05 log|\dot{\varepsilon}| + 0.90)\, {}_sf_y \quad (17) $$

$|\dot{\varepsilon}| \leqq 10^2 \mu/sec$

$$ {}_df_y = {}_sf_y \quad (18) $$

where, ${}_df_y$: yield strength of longitudinal reinforcement (under dynamic loading)

${}_sf_y$: yield strength of longitudinal reinforcement (under static loading)

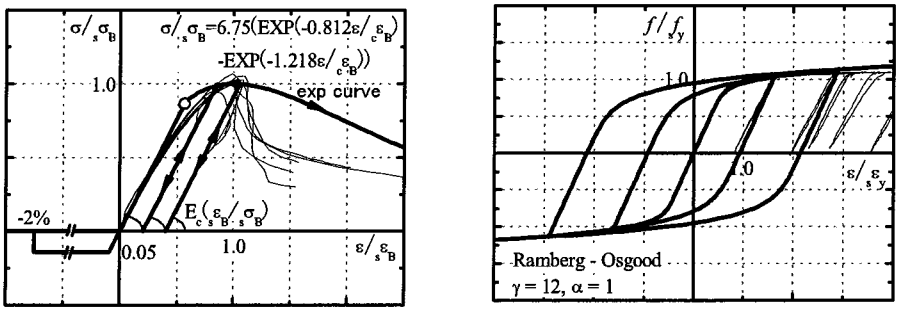

Figure 9. Model of material properties

Results and Discussions

Computed results are compared with those of static loading tests and shaking table tests in Figures 10 and 11, respectively. To verify whether the shapes of hysteresis loop are reproduced, the computed maximum inertia forces Q_{max}, yield stiffness K_y and unloading stiffness K_r are compared with the test results in this section.

(a) Maximum inertia forces Q_{MAX}

As is found in Figure 10, the computed Q_{MAX} under static loading can be reproduced considering the contribution of HPFRCC to tension resistance in Type-S specimen (SS) and neglecting such contribution in Type-P specimen (PS). As is found in Figure 11, the computed Q_{MAX} of both types of specimen (PD and SD) subjected to dynamic loading agrees well with the test result additionally considering the strain rate effects.

(b) Yield-point stiffness and unloading stiffness

The computed yield-point and unloading stiffness of Type-P specimen subjected to both dynamic and static loading shows a better agreement with the test results than that of Type-S specimen and the computed stiffness of Type-S specimen overestimates the test result. This result may be attributed to poor bond behavior of reinforcement due to its relatively large size diameter (diameter 4mm in 30mm

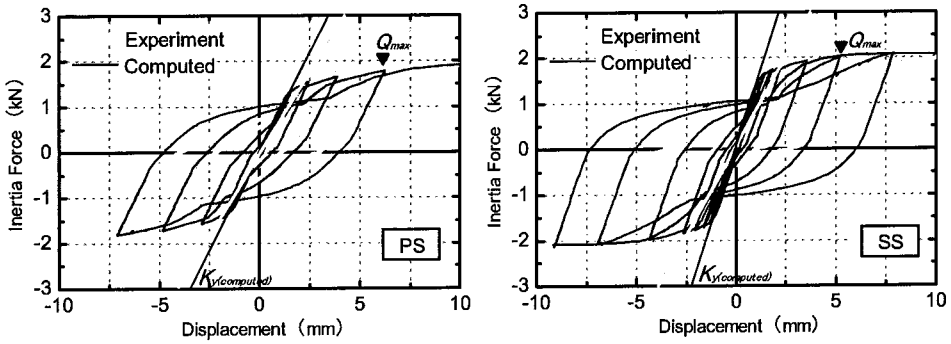

Figure 10. Comparison of computed and static loading test results

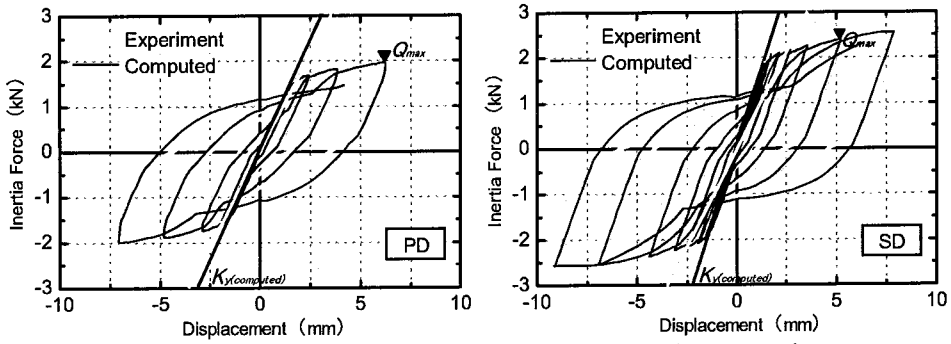

Figure 11. Comparison of computed and dynamic loading test results

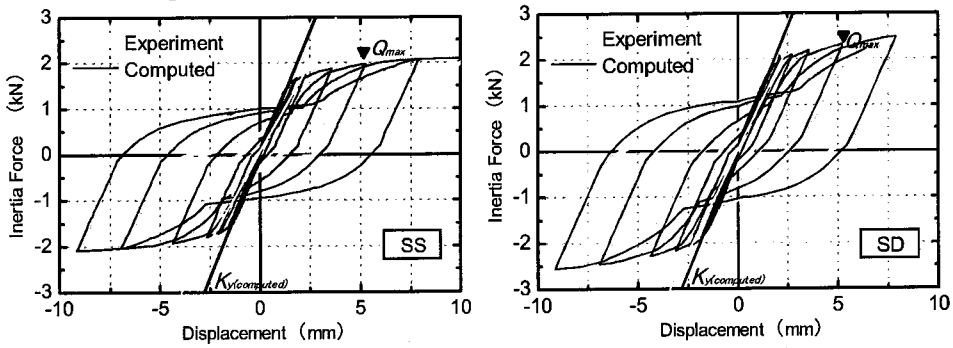

Figure 12. Comparison of computed and test results of Type-S specimen

(20% of the overall displacement is assumed to result from the pull-out behavior of longitudinal reinforcement over the unbonded region)

x 30mm section). Figure 12 shows the comparison of test results and computed results where 20% of the overall displacement of Type-S specimen is assumed to result from the pull-out behavior of longitudinal reinforcement over the unbonded region. As can be found in the figure, the computed yield-point stiffness and unloading stiffness of Type-S specimen agrees better than the results of SS in Figure 10 and SD in Figure 11. It should be noted, however, that the contribution of pull-out behavior to the overall displacement of Type-S specimen may not be clearly determined prior to tests, and the Type-P specimen therefore would be a better candidate to reproduce its behavior through fiber model analyses.

CONCLUSIONS

To establish a simple and cost effective testing technique to simulate seismic behaviors of R/C structures, extremely small-scaled model structures consisting of high performance fiber reinforced cement composite (HPFRCC) material reinforced solely with longitudinal reinforcement are fabricated, and their behaviors are experimentally and analytically investigated.

1) The specimens in this study show ductile behaviors with spindle shaped hysteretic loops and successfully simulates those of typical R/C members.
2) The maximum restoring force Q_{MAX} of Type-S specimen observed in the static loading test is 11% larger than that of Type-P specimen. The observed results can be analytically reproduced considering the contribution of HPFRCC to tension resistance in Type-S specimen and neglecting such contribution in Type-P specimen.
3) The maximum inertia force Q_{MAX} of Type-S specimen observed during the shaking table test is 20% larger than that of Type-P specimen although they have the same sectional and material properties. The computed Q_{MAX} of Type-S and Type-P specimen subjected to dynamic loading agrees well with the experimental result considering the strain rate effects and design details at specimen ends.
4) The computed yield-point and unloading stiffness of Type-P specimen subjected to both dynamic and static loading shows a better agreement with the test results than that of Type-S specimen and the computed stiffness of Type-S specimen overestimates the test result. This result may be attributed to poor bond behavior of reinforcement due to its relatively large size diameter.

ACKNOWLEDGEMENTS

The Central Workshop at the Institute of Industrial Science is greatly appreciated for its technical support in fabricating specimens.

REFERENCES

1. A. E. Naaman and H. W. Reinhardt Ed., High Performance Fiber Reinforced Cement Composites (HPFRCC 2), RILEM Proceeding 31, 1995
2. Sato, Y. Fukuyama, H. Suwada, H.: A Proposal of Tension-Compression Cyclic Loading Test Method for Ductile Cementitious Composite Materials, Journal of Structural and Construction Engineering, No.539, pp. 7-12, Jan., 2001
3. Japanese Industrial Standards Committee, Japanese Industrial Standards B 0205, 1997
4. Noriko T, Yoshiaki N, Yasushi S, Yuki S, Haruhiko S and Hiroshi F.: Shaking Table Test of Small Scaled HPFRCC Column, ERS Bulletin, No.38, pp. 105-118, 2005
5. Hosoya, H. Okada, T. Kitagawa, Y. Nakano, Y. Kumazawa, F.: Fiber Model Analysis of Reinforced Concrete Members with Consideration of The Strain Rate Effect, Journal of Structural and Construction Engineering, No.482, pp. 83-92, Apr., 1996